



OPEN

SUBJECT AREAS:  
CATALYSIS  
GREEN CHEMISTRYReceived  
13 September 2013Accepted  
13 December 2013Published  
13 January 2014Correspondence and  
requests for materials  
should be addressed to  
J.W. (junwang@njut.  
edu.cn)

# $C_3N_4$ - $H_5PMo_{10}V_2O_{40}$ : a dual-catalysis system for reductant-free aerobic oxidation of benzene to phenol

Zhouyang Long, Yu Zhou, Guojian Chen, Weilin Ge &amp; Jun Wang

State Key Laboratory of Materials-Oriented Chemical Engineering, College of Chemistry and Chemical Engineering, Nanjing University of Technology, Nanjing, Jiangsu 210009, P. R. China.

Hydroxylation of benzene is a widely studied atom economical and environmental benign reaction for producing phenol, aiming to replace the existing three-step cumene process. Aerobic oxidation of benzene with  $O_2$  is an ideal and dream process, but benzene and  $O_2$  are so inert that current systems either require expensive noble metal catalysts or wasteful sacrificial reducing agents; otherwise, phenol yields are extremely low. Here we report a dual-catalysis non-noble metal system by simultaneously using graphitic carbon nitride ( $C_3N_4$ ) and Keggin-type polyoxometalate  $H_5PMo_{10}V_2O_{40}$  ( $PMoV_2$ ) as catalysts, showing an exceptional activity for reductant-free aerobic oxidation of benzene to phenol. The dual-catalysis mechanism results in an unusual route to create phenol, in which benzene is activated on the melem unit of  $C_3N_4$  and  $O_2$  by the V-O-V structure of  $PMoV_2$ . This system is simple, highly efficient and thus may lead the one-step production of phenol from benzene to a more practical pathway.

As an important commodity chemical, phenol is industrially produced by the three-step cumene process that suffers from a low one-pass yield *ca.* 5%, high energy cost and large amount of by-products<sup>1,2</sup>. Attempts to overcome these problems prompt the environmental benign one-step processes from benzene to phenol<sup>3-14</sup>, in which the direct oxygenation of benzene to phenol by molecular oxygen ( $O_2$ ) is the most industrially important due to atom economy and economic superiority<sup>5,12</sup>. For decades, various catalysts or catalytic systems have been developed for this aerobic oxidation<sup>2</sup>, including low-temperature liquid-phase reactions<sup>5,9-11</sup>, membrane process<sup>12</sup> and high-temperature gas-phase catalyses<sup>15-17</sup>. However, promoting its practical application remains great challenge because of the very low efficiency of the currently available catalytic systems<sup>2</sup>.

Benzene and  $O_2$  are all inert raw materials in low-temperature liquid-phase reactions. To oxidize benzene to phenol by  $O_2$ , sacrificial reducing agents, *i.e.*  $H_2$ , CO or ascorbic acid, are usually required to generate active oxygen species<sup>2,9</sup>. Otherwise, noble metal catalysts are needed<sup>18-22</sup>, for example, palladium acetate [ $Pd(OAc)_2$ ] with a polyoxometalate (POM) can catalytically convert benzene to phenol in mild liquid-phase aerobic media<sup>18-21</sup>. The utilization of noble metals and/or wasteful reducing agents will largely increase the cost of the catalytic system<sup>2</sup>; therefore, it is very attractive to develop a reductant-free aerobic oxidation of benzene to phenol catalyzed by a non-noble metal catalyst, which is even referred to as a “dream oxidation” in chemical industry<sup>5</sup>.

Here we report a non-noble metal dual-catalysis system  $C_3N_4$ - $H_5PMo_{10}V_2O_{40}$  for efficient aerobic oxidation of benzene to phenol unaided by any reductant. Graphitic carbon nitride ( $C_3N_4$ ) is a low price, insoluble and stable solid material<sup>23</sup>, and we use it as a heterogeneous catalyst for activating benzene chemically<sup>24</sup>. POMs are transition-metal oxygen anion clusters with structural diversity and have been widely used as acid, redox, and bifunctional catalysts<sup>25,26</sup>, among which  $H_5PMo_{10}V_2O_{40}$  ( $PMoV_2$ ) is a V-containing POM well recognized as an efficient homogeneous catalyst for organic oxidations with  $O_2$ <sup>27</sup>. We thus reason that the well dispersion of  $C_3N_4$  in  $PMoV_2$  solution gives rise to a molecular-level contact between them, for which the creation of phenol may be possible from the immediate attack of  $PMoV_2$  catalyst to the already activated benzene ring on  $C_3N_4$  surface. Indeed, the present results prove that the combination of  $C_3N_4$  and  $PMoV_2$  converts benzene to phenol with a high phenol yield in a low-temperature liquid-phase aerobic system without any reductant. A dual-catalysis mechanism is proposed for understanding the highly efficient process.

## Results

The major sample of  $C_3N_4$  employed in this work is designated as  $C_3N_4(580)$ , with the number in the parenthesis indicating the temperature of 580°C for heating melamine in  $C_3N_4$  preparation. We first measured the single



**Table 1 | Aerobic oxidation of benzene over various catalysts. \*Reaction conditions:  $C_3N_4$  0.1 g;  $PMoV_2$  (PMo, PW,  $VOSO_4$ ,  $PMoV_3$ ,  $PMoV_1$  or  $CsPMoV_2$ ) 0.4 g; benzene 4 mL; solvent 25 mL;  $O_2$  2.0 MPa;  $130^\circ C$ ; 4.5 h**

Entry	Catalyst	Solvent	LiOAc (g)	Phenol Yield (%)
1	$C_3N_4(520, 550 \text{ or } 580)$	acetic acid (50 vol.%)	0.6	0
2	$PMoV_2$	acetic acid (50 vol.%)	0.6	0
3	$C_3N_4(580)-PMoV_2$	water (2 mL)	0	2.1
4	$C_3N_4(580)-PMoV_2$	acetic acid (50 vol.%)	0	9.1
5	$C_3N_4(580)-PMoV_2$	acetic acid (50 vol.%)	0.6	13.6
6	melamine- $PMoV_2$	acetic acid (50 vol.%)	0.6	0
7	melem- $PMoV_2$	acetic acid (50 vol.%)	0.6	0
8	$C_3N_4(520)-PMoV_2$	acetic acid (50 vol.%)	0.6	0.3
9	$C_3N_4(550)-PMoV_2$	acetic acid (50 vol.%)	0.6	6.1
10	$C_3N_4(580)-PMo$	acetic acid (50 vol.%)	0.6	0
11	$C_3N_4(580)-PW$	acetic acid (50 vol.%)	0.6	0
12	$C_3N_4(580)-VOSO_4$	acetic acid (50 vol.%)	0.6	0
13	$C_3N_4(580)-PMoV_3$	acetic acid (50 vol.%)	0.6	9.5
14	$C_3N_4(580)-PMoV_1$	acetic acid (50 vol.%)	0.6	0
15	$C_3N_4(580)-CsPMoV_2$	acetic acid (50 vol.%)	0.6	0

catalyst by using  $C_3N_4(580)$  or  $PMoV_2$  alone. Table 1 shows that neither former nor later alone was able to transform benzene in the absence of reductants (entries 1 and 2). On the contrary, a phenol yield of 2.1% was achieved in the dual-catalysis system containing both  $C_3N_4(580)$  and  $PMoV_2$  even with only a small amount of water solvent (2 mL) (Table 1, entry 3). The phenol yield reached 9.1% by changing the solvent to 50 vol.% aqueous solution of acetic acid (Table 1, entry 4), and arose to the maximum value of 13.6% using LiOAc as an effective additive (Table 1, entry 5)<sup>18,20,21</sup>. The above results were obtained at 4.5 h and  $130^\circ C$  optimized from our detailed investigations on various conditions (see Supplementary Fig. S6 online). Many results have been reported on the oxidation of benzene to phenol<sup>5,9–12,15–17</sup>, but reductant-free aerobic oxidation of benzene is still scarcely reported so far. Compared to the previous results under the reductant-free condition, the phenol yield of 13.6% over  $C_3N_4(580)-PMoV_2$  is more than three times higher than the yield of 3.7% over the nano-plate vanadium oxide catalyst at a longer reaction time (10 h) and a higher temperature ( $150^\circ C$ )<sup>28</sup>, and even exceeds the yields on noble metal catalysts [e.g., the homogeneous  $Pd(OAc)_2-PMoV_x$  ( $X = 1, 2, 3$ ) gives the phenol yield around 10%<sup>18,21</sup>, which sharply drops to 3.4% when  $Pd(OAc)_2$  is immobilized on porous supports for recovering<sup>21</sup>]. Moreover, the turnover frequency (TOF) of our work  $5.9 \text{ h}^{-1}$  calculated by the definition  $\text{mmol phenol}/(\text{mmol POM catalyst} \times \text{h reaction time})$  is much higher than the POM-catalyzed systems with CO as the sacrificial reducing agent ( $1.5 \text{ h}^{-1}$ )<sup>5</sup>, or with ascorbic acid as the sacrificial reducing agent ( $0.86 \text{ h}^{-1}$  and  $2.0 \text{ h}^{-1}$ )<sup>10,11</sup>, convincing that our reductant-free cata-

lysis is even more active than those reductant-aided systems. Therefore, the present non-noble metal catalytic system  $C_3N_4(580)-PMoV_2$  shows a remarkably superior efficacy at the reductant-free condition.

Heating melamine in air at high temperatures has been a common approach for preparing  $C_3N_4$ , so the influence of heating temperatures for melamine on this reaction is investigated. The XRD patterns of Fig. 1a shows that heating melamine at  $520^\circ C$  and  $550^\circ C$  led to the formation of graphitic  $C_3N_4$  products of  $C_3N_4(520)$  and  $C_3N_4(550)$ , similar to  $C_3N_4(580)$ , but the low heating temperature  $400^\circ C$  resulted in melem, an intermediate toward  $C_3N_4$ <sup>29,30</sup>. The non- $C_3N_4$ -mediated systems of melamine- $PMoV_2$  and melem- $PMoV_2$  yielded no product (Table 1, entries 6 and 7). Though  $C_3N_4(520)$  and  $C_3N_4(550)$  were also inactive when used alone (Table 1, entry 1), their combination with  $PMoV_2$  gave phenol yields of 0.3% and 6.1%, respectively (Table 1, entries 8 and 9), much lower than 13.6% for  $C_3N_4(580)-PMoV_2$ . The results prove that the  $C_3N_4$  sample obtained at the optimal temperature of  $580^\circ C$  is more active and in favor of the high phenol yield.

We further explored catalytic systems containing  $C_3N_4(580)$  and other POMs. With the V-free POMs, *i.e.*  $H_3PMo_{12}O_{40}$  (PMo) or  $H_3PW_{12}O_{40}$  (PW), to company  $C_3N_4(580)$ , no phenol product appeared (Table 1, entries 10 and 11), suggesting that the V species should be indispensable. Nonetheless,  $C_3N_4(580)$  with the non-POM vanadium species  $VOSO_4$  caused an inactive system either (Table 1, entry 12); as a consequence, it is the V species in POM framework that is synergically active with  $C_3N_4$  for this reaction. Moreover,

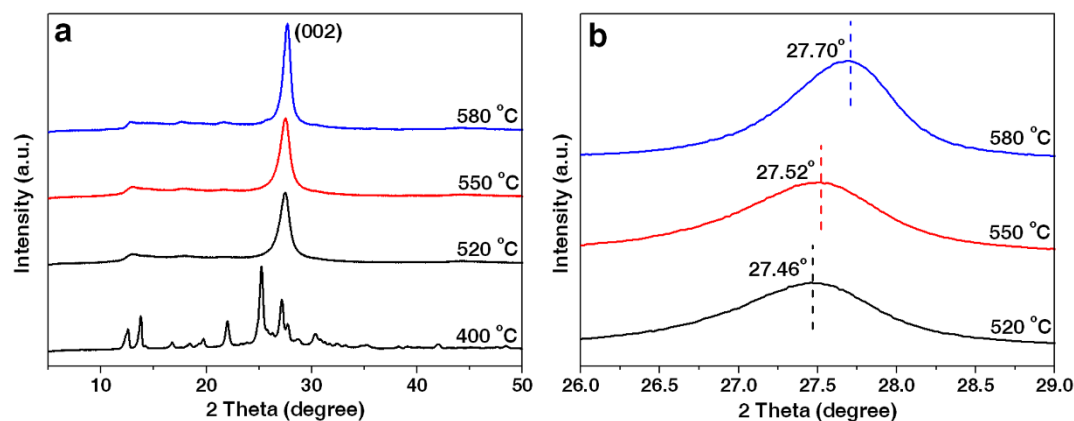


**Figure 1 | (a) XRD patterns for the products by heating melamine at 400, 520, 550 and  $580^\circ C$ ; (b) Magnification of the peak (002) in the  $2\theta$  range  $26 \sim 29^\circ$  for the  $C_3N_4$  products obtained at 520, 550 and  $580^\circ C$ .**



when the other two less frequently used V-containing POMs (PMoV<sub>1</sub> and PMoV<sub>3</sub>) were tested, the results show that C<sub>3</sub>N<sub>4</sub>(580)-PMoV<sub>3</sub> exhibited comparable activity to C<sub>3</sub>N<sub>4</sub>(580)-PMoV<sub>2</sub>, but C<sub>3</sub>N<sub>4</sub>(580)-PMoV<sub>1</sub> was definitely inactive (Table 1, entries 13 and 14), which means that not all the V species in POM framework can catalyze this reaction with C<sub>3</sub>N<sub>4</sub>.

## Discussion

According to previous studies, the V species in V-POMs are well accepted as the catalytically active sites for versatile organic oxidations<sup>31</sup>. Particularly, for liquid-phase aerobic oxidations, PMoV<sub>2</sub> takes a catalytic effect through Mars-van Krevelen-type mechanism, where the lattice oxygen of PMoV<sub>2</sub> selectively oxygenates organic substrates *via* a valence variation between V<sup>5+</sup> and V<sup>4+</sup><sup>27,32</sup>. Neumann and co-workers<sup>27,32–35</sup> have systematically studied series of PMoV<sub>2</sub>-catalyzed homogeneous oxidations, and based on the Mars-van Krevelen mechanism they propose that the isomers of PMoV<sub>2</sub> with vanadium atoms in adjacent positions (*i.e.* V-O-V structure) are more likely to form bridge defects, favoring higher activity in oxygen-transfer reactions. Therefore, only PMoV<sub>2</sub> and PMoV<sub>3</sub> with the highly active V-O-V structure in their frameworks can allow the occurrence of oxygen transfer in hydroxylation of benzene to phenol, while lack of V-O-V is responsible for the inactivity of PMoV<sub>1</sub>.

Nonetheless, PMoV<sub>2</sub> or PMoV<sub>3</sub> alone cannot catalyze the reaction because of inertness of the substrate benzene, suggesting that C<sub>3</sub>N<sub>4</sub> should play a key role. Recently, Goettmann *et al.*<sup>24,36</sup> conclude an unusual activation of aromatic rings *via* transferring electron density from the melem unit of C<sub>3</sub>N<sub>4</sub> to arene based on reaction results plus DFT calculations. Besides, for the high-temperature gas-phase oxidation of benzene with O<sub>2</sub> over copper exchanged HZSM5, a bifunctional catalytic mechanism has been reported: phenol is produced from the simultaneous activation of benzene and O<sub>2</sub> on zeolitic acid and Cu metal sites, respectively<sup>16,17</sup>. From above analyses, a dual-catalysis mechanistic pathway is proposed for understanding the catalytic performance of C<sub>3</sub>N<sub>4</sub>-PMoV<sub>2</sub> in Fig. 2. Benzene is firstly catalytically activated by the melem unit of graphitic C<sub>3</sub>N<sub>4</sub>, forming a transitional intermediate of electron-enriched benzene ring. Immediately, the original oxidation state of PMoV<sub>2</sub> with V<sup>5+</sup> species, designated as PMoV<sub>2</sub><sup>[ox]</sup>, attacks the intermediate ring to produce phenol, wherein the lattice oxygen of a V-O-V structure in PMoV<sub>2</sub><sup>[ox]</sup> moves into the benzene ring with the PMoV<sub>2</sub><sup>[ox]</sup> thus being reduced to the V<sup>4+</sup>-containing PMoV<sub>2</sub><sup>[red]</sup>. Finally, the catalytic cycle is closed with the resume of PMoV<sub>2</sub><sup>[ox]</sup> after O<sub>2</sub> re-oxidizes V<sup>4+</sup> of PMoV<sub>2</sub><sup>[red]</sup> into V<sup>5+</sup> species.

In the dual-catalysis mechanism above, the role of C<sub>3</sub>N<sub>4</sub> is activating benzene according to the previous finding that the  $\pi$ -conju-

gated melem unit of C<sub>3</sub>N<sub>4</sub> could transfer electron density to aromatic rings<sup>24,36</sup>. It is further revealed that high temperatures for thermal condensation of melamine would enhance the  $\pi$ -conjugation by connecting more tri-s-triazine and extending the polymeric network of C<sub>3</sub>N<sub>4</sub><sup>37</sup>. The (002) diffraction peak of C<sub>3</sub>N<sub>4</sub> is assigned to the inter-layer distance of its graphitic structure<sup>30</sup>. In our case, as shown in the magnification of XRD patterns in Fig. 1b, the gradual shifting of the (002) peak to larger degrees along with the raise of heating temperatures means the shortening of the stacking distance and thus the stronger overlap of  $\pi$  orbital in C<sub>3</sub>N<sub>4</sub><sup>29,30</sup>, indicating that the activation of benzene would be improved by a higher heating temperature up to 580 °C. This accounts for the activity order C<sub>3</sub>N<sub>4</sub>(520)-PMoV<sub>2</sub> < C<sub>3</sub>N<sub>4</sub>(550)-PMoV<sub>2</sub> < C<sub>3</sub>N<sub>4</sub>(580)-PMoV<sub>2</sub>. On the other hand, melem-PMoV<sub>2</sub> is inactive because melem itself has no graphitic characteristic of C<sub>3</sub>N<sub>4</sub><sup>30</sup>.

Also according to the mechanism in Fig. 2, the catalyst PMoV<sub>2</sub> will remain in its reduced state PMoV<sub>2</sub><sup>[red]</sup> as the reaction occurs in O<sub>2</sub>-deficient environment. Thus we conducted a separate run by introducing a much less amount of O<sub>2</sub> (0.3 MPa) (see Supplementary Information) into the batch reactor. In this case, the recovered PMoV<sub>2</sub> was green and exhibited an eight-line signal in ESR spectra (Fig. 3), index of the reduced state PMoV<sub>2</sub><sup>[red]</sup><sup>5,10</sup>, whereas the fresh and recovered PMoV<sub>2</sub> from O<sub>2</sub>-sufficient condition were orange and ESR silent, denoting the oxidation state PMoV<sub>2</sub><sup>[ox]</sup>. The above phenomena and comparisons strongly evidence our proposal that there exists V<sup>5+</sup>/V<sup>4+</sup> switch during the reaction.

Moreover, the activation and oxidation of benzene should occur simultaneously in this mechanism. In order to reflect this point, the well-known heterogeneous Cs salt of PMoV<sub>2</sub>, CsPMoV<sub>2</sub><sup>10</sup>, was tried as a partner with C<sub>3</sub>N<sub>4</sub>(580). Though CsPMoV<sub>2</sub> was as active as PMoV<sub>2</sub> (see Supplementary Table S1 online)<sup>10</sup> in the presence of the sacrificial reducing agent ascorbic acid, C<sub>3</sub>N<sub>4</sub>(580)-CsPMoV<sub>2</sub> was inactive in our reaction system (Table 1, entry 15). The SEM image for CsPMoV<sub>2</sub> (see Supplementary Fig. S5 online) shows a spherical morphology with spheres diameters being 800 ~ 900 nm. This bulk CsPMoV<sub>2</sub> may not contact well with another solid surface of C<sub>3</sub>N<sub>4</sub>(580), hindering the simultaneous attachment of substrate with the dual-catalyst. In other words, the intimate and efficient contacts among C<sub>3</sub>N<sub>4</sub>, benzene and PMoV<sub>2</sub> are essential for implementing the overall catalytic cycle, which further supports our mechanism.

Besides benzene, the simplest alkyl aromatic molecule toluene was also attempted as the substrate to further investigate the catalytic behavior of C<sub>3</sub>N<sub>4</sub>(580)-PMoV<sub>2</sub> for aerobic oxidation of aromatic rings (see Supplementary Table S2 online). C<sub>3</sub>N<sub>4</sub>(580) alone was

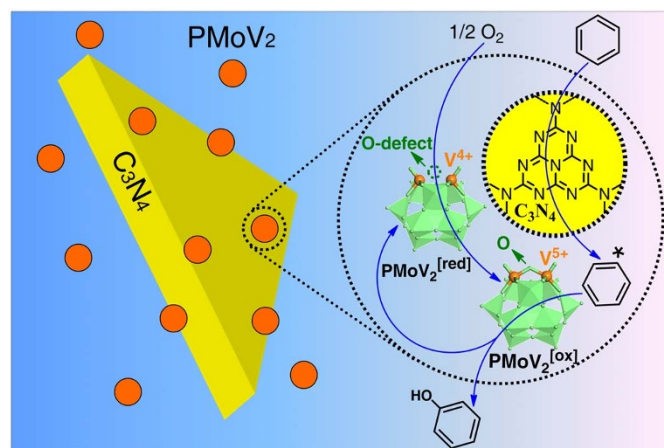


**Figure 2** | Proposed mechanistic pathway for C<sub>3</sub>N<sub>4</sub>-PMoV<sub>2</sub>-catalyzed aerobic oxidation of benzene to phenol.

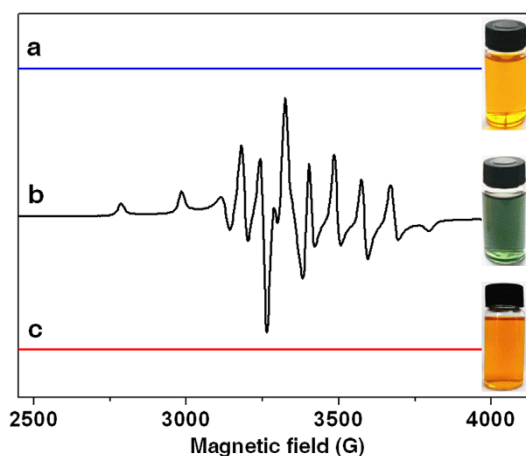


**Figure 3** | ESR spectra of (a) fresh PMoV<sub>2</sub>, (b) recycled PMoV<sub>2</sub> from the O<sub>2</sub>-insufficient reaction, and (c) recycled PMoV<sub>2</sub> from the O<sub>2</sub>-sufficient reaction, entry 1 of Table 1.





inert in this system, and yet, bare  $\text{PMoV}_2$  exclusively produced methyl-oxygenated compounds of benzaldehyde (7.7%) and benzyl alcohol (1.4%) due to the side chain oxidations. For reductant-free oxidations of alkyl aromatics, early studies reveal that oxidations of benzylic C-H bond are preferred rather than the aromatic ring<sup>9,38,39</sup>. On the contrary, the dual-catalysis system  $\text{C}_3\text{N}_4(580)\text{-PMoV}_2$  resulted in a desirable yield of cresols (0.4%) due to the ring oxidation. This feature suggests that  $\text{C}_3\text{N}_4\text{-PMoV}_2$  should have enhanced the reactivity of the alkylated benzene ring, enabling occurrence of the ring oxygenation through the dual-catalysis mechanism in Fig. 1.

Catalytic reusability was first investigated by recycling  $\text{C}_3\text{N}_4(580)$  alone (Fig. 4). The phenol yield slowly decreased from 13.6% for the fresh catalyst to 12.7% for 1<sup>st</sup>, 9.8% for 2<sup>nd</sup>, and still kept at 6.2% for 3<sup>rd</sup> recycling. The XRD pattern for the last recycled  $\text{C}_3\text{N}_4(580)$  indicates a stable structural stability due to its identical diffraction peak to that of the fresh one (see Supplementary Fig. S1 online). Therefore, the above decrease of phenol yield can be ascribed to the tar deposition according to the gradually darkened color (inserted photos in Fig. 4) and variation of C content (see Supplementary Information) of  $\text{C}_3\text{N}_4(580)$  during the recycling process. In fact, tar is still an inevitable over-oxidation byproduct, because the main product phenol is more reactive than the substrate benzene<sup>4,6,18</sup>. Even so, when  $\text{C}_3\text{N}_4(580)$ ,  $\text{PMoV}_2$  and  $\text{LiOAc}$  were simultaneously recovered (see Methods), the phenol yield was 10.3% and 6.5% for the 1<sup>st</sup> and 2<sup>nd</sup> recycling, and still 2.1% for the 3<sup>rd</sup> recycling (Fig. 4).

All the above results demonstrate that the dual-catalysis non-noble metal system  $\text{C}_3\text{N}_4\text{-PMoV}_2$  provides a high phenol yield of 13.6% in reductant-free aerobic oxidation of benzene. A dual-catalysis mechanism involving cooperative activations of benzene on melem unit of  $\text{C}_3\text{N}_4$  and  $\text{O}_2$  by V-O-V structure of  $\text{PMoV}_2$  is demonstrated for interpreting catalytic results. The present dual-catalysis process appears to be simpler, much more efficient and cost-effective when compared with the currently available catalytic systems, paving a promising step towards practical application of hydroxylation of benzene to phenol by molecular oxygen.

## Methods

**Materials and general methods.** All chemicals were analytical grade and used as received.  $\text{H}_3\text{PMo}_{10}\text{V}_2\text{O}_{40}$  (PMo) and  $\text{H}_3\text{PW}_{12}\text{O}_{40}$  (PW), purchased commercially, were dried before used. XRD patterns were collected on the Bruker D8 Advance powder diffractometer using Ni-filtered Cu K $\alpha$  radiation source at 40 kV and 20 mA, from 5 to 50° with a scan rate of 0.2° S<sup>-1</sup>, and before measurements the samples were dried at 100°C for 2 h. Elemental analyses were performed on a CHN elemental analyzer (FlashEA 1112). BET surface areas were calculated from the sorption isotherms measured at the temperature of liquid nitrogen using a Micromeritics ASAP2010 analyzer; the samples were degassed at 300°C to a vacuum of 10<sup>-3</sup> Torr before analysis. FT-IR spectra were recorded on a Nicolet 360 FT-IR instrument (KBr discs) in the 4,000–400 cm<sup>-1</sup> region. ESR spectra were recorded on a Bruker EMX-10/12

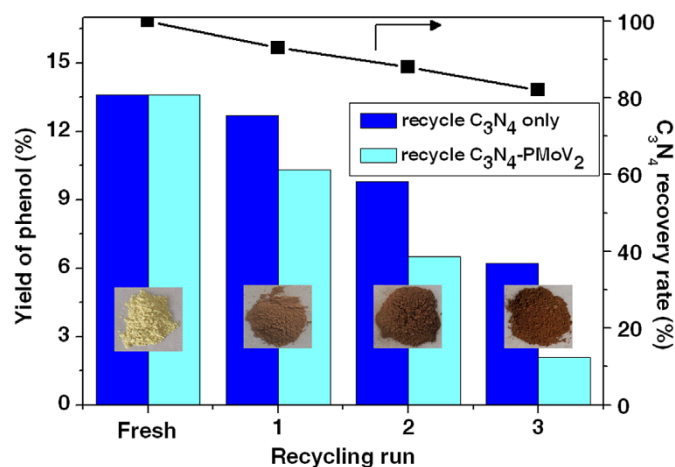


**Figure 4** | Phenol yields and  $\text{C}_3\text{N}_4$  recovery rate during the recycling test; insertion:  $\text{C}_3\text{N}_4$  photo for each run.

spectrometer at X-band. The measurements were done at  $-110^\circ\text{C}$  in a frozen solution provided by a liquid/gas nitrogen temperature regulation system controlled by a thermocouple located at the bottom of the microwave cavity within a Dewar insert.

**Preparation of catalysts.** Graphitic carbon nitride ( $\text{C}_3\text{N}_4$ ). The procedure for the synthesis of  $\text{C}_3\text{N}_4(580)$  is similar to the previous reports<sup>40,41</sup>. Melamine was transferred into a crucible and heated in a muffle furnace under air at a rate of 15°C/min to reach the temperature of 580°C and kept at 580°C for 4 h, then the resulting yellow sample was cooled to room temperature in the oven. Melem,  $\text{C}_3\text{N}_4(520)$  and  $\text{C}_3\text{N}_4(550)$  were prepared by the similar method at 400°C, 520°C and 550°C, respectively.

$\text{H}_3\text{PMo}_{10}\text{V}_2\text{O}_{40}$  ( $\text{PMoV}_2$ ). The Keggin-structured double V-containing POM was prepared according to the procedure described in our previous report<sup>42</sup>. The detail of the preparation of  $\text{PMoV}_2$  procedure is as the following.  $\text{MoO}_3$  (16.59 g) and  $\text{V}_2\text{O}_5$  (2.1 g) were added to deionized water (250 mL). The mixture was heated up to the reflux temperature under vigorously stirring with a water-cooled condenser, then at 120°C the 85 wt% aqueous solution of  $\text{H}_3\text{PO}_4$  (1.33 g) was added drop-wise to the reaction mixture. When a clear orange-red solution appeared, it was cooled to room temperature. The orange-red powder  $\text{PMoV}_2$  was obtained by evaporation of the solution to dryness, followed with re-crystallizing for purification.

$\text{Cs}_3\text{PMo}_{10}\text{V}_2\text{O}_{40}$  ( $\text{CsPMoV}_2$ ) was prepared according to the literature<sup>10</sup>, with  $\text{Cs}_2\text{CO}_3$  instead of  $\text{CsNO}_3$ . FT-IR spectrum for  $\text{CsPMoV}_2$  is presented in Fig. S4b.

**Catalytic tests.** The hydroxylation of benzene was carried out in 100 ml stainless steel autoclave equipped with a mechanical stirrer and an automatic temperature controller. In a typical test, 0.1 g  $\text{C}_3\text{N}_4$ , 0.4 g  $\text{PMoV}_2$ , 0.6 g  $\text{LiOAc}$ , and 4.0 mL benzene were added into 25 mL of the aqueous solution of acetic acid (50 vol%) successively. After the system was charged with 2.0 MPa  $\text{O}_2$  at room temperature, the hydroxylation reaction was conducted at 130°C K for 4.5 h with vigorous stirring. After the reaction, 1, 4-dioxane was added into the product mixture as an internal standard for product analysis. The mixture was analyzed by a gas chromatograph (GC) with a FID and a capillary column (SE-54; 30 m  $\times$  0.32 mm  $\times$  0.25  $\mu\text{m}$ ). Yield of phenol was calculated as mmol phenol/mmol initial benzene. Catechol, hydroquinone and benzoquinone were not detected by our GC analysis, so the tar that cannot be detected by the GC technique was the over-oxidation product.

**Recycling of the catalyst system.** After the reaction, the reaction mixture was centrifuged and the solid  $\text{C}_3\text{N}_4(580)$  was recovered, followed by washing with acetic acid and dried in vacuum, and then reused in the next run. After the solid  $\text{C}_3\text{N}_4(580)$  was separated by centrifuging, water was added into the left liquid phase followed by extraction with isopropyl ether. The combined aqueous extracts were filtered and concentrated by evaporation under reduced pressure. The resulting solid mixture containing used  $\text{PMoV}_2$  and  $\text{LiOAc}$  was obtained.

- Panov, G. I. Advances in oxidation catalysis; oxidation of benzene to phenol by nitrous oxide. *CATTECH* **4**, 18–31 (2000).
- Antonyraj, C. A. & Kannan, S. One-step hydroxylation of benzene to phenol over layered double hydroxides and their derived forms. *Catal. Surv. Asia* **17**, 47–70 (2013).
- Tanev, P. T., Chibwe, M. T. & Pinnavaia, J. Titanium-containing mesoporous molecular sieves for catalytic oxidation of aromatic compounds. *Nature* **368**, 321–323 (1994).
- Balducci, L. *et al.* Direct oxidation of benzene to phenol with hydrogen peroxide over a modified titanium silicalite. *Angew. Chem. Int. Ed.* **42**, 4937–4940 (2003).
- Tani, M., Sakamoto, T., Mita, S., Sakaguchi, S. & Ishii, Y. Hydroxylation of benzene to phenol under air and carbon monoxide catalyzed by molybdovanadophosphoric acid. *Angew. Chem. Int. Ed.* **44**, 2586–2588 (2005).
- Chen, X. F., Zhang, J. S., Fu, X. Z., Antonietti, M. & Wang, X. C. Fe-g- $\text{C}_3\text{N}_4$ -catalyzed oxidation of benzene to phenol using hydrogen peroxide and visible light. *J. Am. Chem. Soc.* **131**, 11658–11659 (2009).
- Ide, Y., Matsuoka, M. & Ogawa, M. Efficient visible-light-induced photocatalytic activity on gold-nanoparticle-supported layered titanate. *J. Am. Chem. Soc.* **132**, 16762–16764 (2010).
- Lee, B., Naito, H. & Hibino, T. Electrochemical oxidation of benzene to phenol. *Angew. Chem. Int. Ed.* **51**, 440–444 (2012).
- Punniyamurthy, T., Velusamy, S. & Iqbal, J. Recent advances in transition metal catalyzed oxidation of organic substrates with molecular oxygen. *Chem. Rev.* **105**, 2329–2363 (2005).
- Yamaguchi, S., Sumimoto, S., Ichihashi, Y., Nishiyama, S. & Tsuruya, S. Liquid-phase oxidation of benzene to phenol over V-substituted heteropolyacid catalysts. *Ind. Eng. Chem. Res.* **44**, 1–7 (2005).
- Liu, Y. Y., Murata, K. & Inaba, M. Liquid-phase oxidation of benzene to phenol by molecular oxygen over transition metal substituted polyoxometalate compounds. *Catal. Commun.* **6**, 679–683 (2005).
- Niwa, S. *et al.* A one-step conversion of benzene to phenol with a palladium membrane. *Science* **295**, 105–107 (2002).
- Fu, M., Satoh, Y. & Osa, T. Heterogeneous photocatalytic oxidation of aromatic compounds on  $\text{TiO}_2$ . *Nature* **293**, 206–208 (1981).



14. Ohkubo, K., Kobayashi, T. & Fukuzumi, S. Direct oxygenation of benzene to phenol using quinolinium ions as homogeneous photocatalysts. *Angew. Chem. Int. Ed.* **50**, 8652–8655 (2011).
15. Tada, M. *et al.* In situ time-resolved DXAFS for the determination of kinetics of structural changes of H-ZSM-5-supported active Re-cluster catalyst in the direct phenol synthesis from benzene and O<sub>2</sub>. *Phys. Chem. Chem. Phys.* **12**, 5701–5706 (2010).
16. Tabler, A., Häusser, A. & Roduner, E. Aerobic one-step oxidation of benzene to phenol on copper exchanged HZSM5 zeolites: a mechanistic study. *J. Mol. Catal. A Chem.* **379**, 139–145 (2013).
17. Kromer, A. & Roduner, E. Catalytic oxidation of benzene on liquid ion-exchanged Cu, H (Na)/ZSM-5 and Cu, H (Na)/Y zeolites: spin trapping of transient radical intermediates. *ChemPlusChem* **78**, 268–273 (2013).
18. Passoni, L. C., Cruz, A. T., Buffon, R. & Schuchardt, U. Direct selective oxidation of benzene to phenol using molecular oxygen in the presence of palladium and heteropolyacids. *J. Mol. Catal. A Chem.* **120**, 117–123 (1997).
19. Passoni, L. C., Luna, F. J., Wallau, M., Buffon, R. & Schuchardt, U. Heterogenization of H<sub>6</sub>PMo<sub>9</sub>V<sub>3</sub>O<sub>40</sub> and palladium acetate in VPI-5 and MCM-41 and their use in the catalytic oxidation of benzene to phenol. *J. Mol. Catal. A Chem.* **134**, 229–235 (1998).
20. Burton, H. A. & Kozhevnikov, I. V. Biphasic oxidation of arenes with oxygen catalysed by Pd(II)–heteropoly acid system: oxidative coupling versus hydroxylation. *J. Mol. Catal. A Chem.* **185**, 285–290 (2002).
21. Liu, Y. Y., Murata, K. & Inaba, M. Direct oxidation of benzene to phenol by molecular oxygen over catalytic systems containing Pd(OAc)<sub>2</sub> and heteropolyacid immobilized on HMS or PIM. *J. Mol. Catal. A Chem.* **256**, 247–255 (2006).
22. Murata, K., Liu, Y. Y. & Inaba, M. Effects of vanadium supported on ZrO<sub>2</sub> and sulfolane on the synthesis of phenol by hydroxylation of benzene with oxygen and acetic acid on palladium catalyst. *Catal. Lett.* **102**, 143–147 (2005).
23. Wang, Y., Wang, X. C. & Antonietti, M. Polymeric graphitic carbon nitride as a heterogeneous organocatalyst: from photochemistry to multipurpose catalysis to sustainable chemistry. *Angew. Chem. Int. Ed.* **51**, 68–89 (2012).
24. Goettmann, F., Fischer, A., Antonietti, M. & Thomas, A. Chemical synthesis of mesoporous carbon nitrides using hard templates and their use as a metal-free catalyst for friedel–crafts reaction of benzene. *Angew. Chem. Int. Ed.* **45**, 4467–4471 (2006).
25. Kozhevnikov, I. V. Catalysis by heteropoly acids and multicomponent polyoxometalates in liquid-phase reactions. *Chem. Rev.* **98**, 171–198 (1998).
26. Leng, Y. *et al.* Heteropolyanion-based ionic liquids: reaction-induced self-separation catalysts for esterification. *Angew. Chem., Int. Ed.* **48**, 168–171 (2009).
27. Neumann, R. Activation of molecular oxygen, polyoxometalates, and liquid-phase catalytic oxidation. *Inorg. Chem.* **49**, 3594–3601 (2010).
28. Gao, X. H., Lv, X. C. & Xu, J. Oxidation of benzene to phenol by dioxygen over vanadium oxide nano-plate. *Kinet. Catal.* **51**, 394–397 (2010).
29. Tyborski, T. *et al.* Tunable optical transition in polymeric carbon nitrides synthesized via bulk thermal condensation. *J. Phys.: Condens. Matter* **24**, 162201–162204 (2012).
30. Thomas, A. *et al.* Graphitic carbon nitride materials: variation of structure and morphology and their use as metal-free catalysts. *J. Mater. Chem.* **18**, 4893–4908 (2008).
31. Mizuno, N., Kamata, K. & Yamaguchi, K. Liquid-phase selective oxidation by multimetallic active sites of polyoxometalate-based molecular catalysts. *Top. Organomet. Chem.* **37**, 127–160 (2011).
32. Khenkin, A. M., Weiner, L., Wang, Y. & Neumann, R. Electron and oxygen transfer in polyoxometalate, H<sub>5</sub>PV<sub>2</sub>Mo<sub>10</sub>O<sub>40</sub>, Catalyzed oxidation of aromatic and alkyl aromatic compounds: evidence for aerobic Mars-van Krevelen-type reactions in the liquid homogeneous phase. *J. Am. Chem. Soc.* **123**, 8531–8542 (2001).
33. Khenkin, A. M. & Neumann, R. Low-temperature activation of dioxygen and hydrocarbon oxidation catalyzed by a phosphovanadomolybdate: evidence for Mars-van Krevelen-type mechanism in a homogeneous liquid phase. *Angew. Chem. Int. Ed.* **39**, 4088–4090 (2000).
34. Efremenko, I. & Neumann, R. Protonation of phosphovanadomolybdates H<sub>3+x</sub>PV<sub>x</sub>Mo<sub>12-x</sub>O<sub>40</sub>: computational insight into reactivity. *J. Phys. Chem. A* **115**, 4811–4826 (2011).
35. Efremenko, I. & Neumann, R. Computational insight into the initial steps of the Mars–van Krevelen mechanism: electron transfer and surface defects in the reduction of polyoxometalates. *J. Am. Chem. Soc.* **134**, 20669–20680 (2012).
36. Goettmann, F., Thomas, A. & Antonietti, M. Metal-free activation of CO<sub>2</sub> by mesoporous graphitic carbon nitride. *Angew. Chem. Int. Ed.* **46**, 2717–2720 (2007).
37. Zhang, Y. *et al.* Synthesis and luminescence mechanism of multicolor-emitting g-C<sub>3</sub>N<sub>4</sub> nanopowders by low temperature thermal condensation of melamine. *Sci. Rep.* **3**, 1943; DOI:10.1038/srep01943 (2013).
38. Kesavan, L. *et al.* Solvent-free oxidation of primary carbon-hydrogen bonds in toluene using Au-Pd alloy nanoparticles. *Science* **331**, 195–199 (2011).
39. Li, X. H., Wang, X. & Antonietti, M. Solvent-free and metal-free oxidation of toluene using O<sub>2</sub> and g-C<sub>3</sub>N<sub>4</sub> with nanopores: nanostructure boosts the catalytic selectivity. *ACS Catal.* **2**, 2082–2086 (2012).
40. Yan, S. C., Li, Z. S. & Zou, Z. G. Photodegradation performance of g-C<sub>3</sub>N<sub>4</sub> fabricated by directly heating melamine. *Langmuir* **25**, 10397–10401 (2009).
41. Dong, F. *et al.* Efficient synthesis of polymeric g-C<sub>3</sub>N<sub>4</sub> layered materials as novel efficient visible light driven photocatalysts. *J. Mater. Chem.* **21**, 15171–15174 (2011).
42. Zhao, P. P. *et al.* A polyoxometalate-based Pd<sup>II</sup>-coordinated ionic solid catalyst for heterogeneous aerobic oxidation of benzene to biphenyl. *Chem. Commun.* **48**, 5721–5723 (2012).

## Acknowledgments

We thank the National Natural Science Foundation of China (Nos. 21136005 and 21303084), Jiangsu Province Science Foundation for Youths (No. BK20130921), and Scientific Research and Innovation Project for College Graduates of Jiangsu Province (CXZZ13\_0442).

## Author contributions

Z.Y.L. and J.W. conceived and designed the experiments. Z.Y.L. performed all the experiments and analyzed all the data. G.J.C. and W.L.G. performed catalysts characterization. Z.Y.L., Y.Z. and J.W. co-wrote the paper. All the authors discussed the results and commented on the manuscript.

## Additional information

Supplementary information accompanies this paper at <http://www.nature.com/scientificreports>

**Competing financial interests:** The authors declare no competing financial interests.

**How to cite this article:** Long, Z.Y., Zhou, Y., Chen, G.J., Ge, W.L. & Wang, J. C<sub>3</sub>N<sub>4</sub>-H<sub>5</sub>PMo<sub>10</sub>V<sub>2</sub>O<sub>40</sub>: a dual-catalysis system for reductant-free aerobic oxidation of benzene to phenol. *Sci. Rep.* **4**, 3651; DOI:10.1038/srep03651 (2014).



This work is licensed under a Creative Commons Attribution-NonCommercial-NoDerivs 3.0 Unported license. To view a copy of this license, visit <http://creativecommons.org/licenses/by-nc-nd/3.0>